Feasibility studies for hydrogen reduction of ilmenite in a static system for use as an ISRU demonstration on the lunar surface

Journal Item

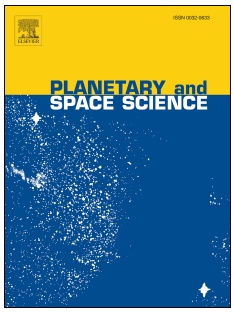

Feasibility studies for hydrogen reduction of ilmenite in a static system for use as an ISRU demonstration on the lunar surface

H.M. Sargeant, F.A.J. Abernethy, M. Anand, S.J. Barber, P. Landsberg, S. Sheridan, I. Wright, A. Morse

PII: S0032-0633(18)30400-8

DOI: https://doi.org/10.1016/j.pss.2019.104759

Reference: PSS 104759

To appear in: *Planetary and Space Science*

Received Date: 6 November 2018

Revised Date: 11 September 2019

Accepted Date: 26 September 2019

Please cite this article as: Sargeant, H.M., Abernethy, F.A.J., Anand, M., Barber, S.J., Landsberg, P., Sheridan, S., Wright, I., Morse, A., Feasibility studies for hydrogen reduction of ilmenite in a static system for use as an ISRU demonstration on the lunar surface, *Planetary and Space Science* (2019), doi: https://doi.org/10.1016/j.pss.2019.104759.

Feasibility Studies for Hydrogen Reduction of Ilmenite in a Static System for use as an ISRU Demonstration on the Lunar Surface

H.M. Sargeant[1], F.A.J. Abernethy[1], M. Anand[1,2], S.J Barber[1], P. Landsberg[1], S. Sheridan[1], I. Wright[1], A. Morse[1].

[1]School of Physical Sciences, The Open University, Milton Keynes MK7 6AA, UK.

[2]Department of Earth Sciences, The Natural History Museum, London, SW7 5BD, UK.

Corresponding author: Hannah Sargeant (hannah.sargeant@open.ac.uk)

Abstract

The ESA-ROSCOSMOS mission, Luna-27, scheduled for launch in 2023, includes a payload known as PROSPECT that is intended for sampling the polar lunar regolith through drilling, with subsequent analyses of the retrieved material. One of the aims of the analytical module, ProSPA, which is being developed at The Open University, is to identify and quantify the volatiles present in the extracted sample that are released by heating from ambient up to 1000 °C and analyzed by the mass spectrometers to assess their potential for in-situ resource utilization. The ProSPA design also includes a provision to test the extraction of water (and its associated oxygen) from lunar regolith by hydrogen reduction. Previous attempts at such extractions generally utilize a flow of hydrogen gas through the feedstock to efficiently extract water. However, in ProSPA, samples would be processed in a static mode, which leads to concerns that the reaction may be suppressed by inefficient removal of water vapor above the regolith. A first order theoretical assessment of the diffusion of

gases in such a system was performed and suggested that water can diffuse through the system at an acceptable rate and be collected upon a cold finger thus enabling the reaction to proceed. Proof of concept experiments were successfully performed with a ProSPA breadboard using ilmenite samples up to ~45 mg heated at 900 °C for 60 minutes. Subsequent heating of the cold finger, in vacuum, released 17±1 μmol water from a 44.7±0.5 mg sample, equating to a calculated yield of 0.6±0.1 wt. % oxygen, and a reduction extent of 5.8±0.4 %. A sample of mass 11.2±0.5 mg had the greatest calculated yield of 1.4±0.2 wt. % oxygen, and this equates to a reduction extent of 12.9±1.5 %. SEM analyses of cross-sections of grains showed evidence of a reduction reaction inside the ilmenite grains with some showing greater reduction than others, indicating the reaction is limited by furnace dimensions, reaction kinetics and geometry. The results suggest that the ProSPA ISRU experiment should be capable of producing water, and therefore oxygen, by hydrogen reduction of ilmenite, ultimately this could be a viable technique for producing oxygen from ilmenite-containing lunar regolith with ProSPA.

Keywords

#ISRU #Ilmenite #Hydrogen Reduction #PROSPECT #ProSPA #Moon

Highlights

- Hydrogen gas can reduce ilmenite in a ProSPA-type system to produce water
- Water can be condensed and released for quantification using a cold finger
- The ProSPA ISRU experiment is a useful prospecting technique

1 Introduction

In Situ Resource Utilization (ISRU) is the concept of harvesting local resources, resulting in space exploration missions that would ultimately be more cost-effective than those solely reliant on the transport of resources from the Earth. Although theoretical ISRU studies have been undertaken from as early as 1979 (Rao et al., 1979), more attention has been paid to laboratory and field studies in the last decade (e.g. Sanders & Larson, 2012) as such technologies could enable future long term exploration missions to the Moon and Mars (ESA, 2015; ISECG, 2018).

The ambition to develop a long-term sustainable presence in space has spurred the proposal, study and development of a number of ISRU demonstration and resource prospecting instruments. Examples of such technologies include ROxygen and PILOT (Pre-cursor ISRU Lunar Oxygen Testbed) which both perform hydrogen reduction of regolith with yields of 1-2 wt.% oxygen production from regolith. The RESOLVE (Regolith and Environmental Science and Oxygen and Lunar Volatile Extraction) instrument looks for volatiles in permanently shadowed regions as well as performing hydrogen reduction of regolith (Sanders and Larson, 2011, 2012). The Mars Oxygen In-Situ Resource Utilization Experiment, MOXIE, is a payload on the Mars 2020 rover

which will extract oxygen from the Martian atmosphere (Meyen et al., 2016). The European Space Agency (ESA) has committed to performing a lunar ISRU demonstration mission by 2025 (ESA, 2018). Such a mission will build on findings highlighted at the European-wide ISRU workshop (Anand et al., 2018), and research performed in European institutions (e.g. Denk, 2018; Lomax et al., 2019). The primary ISRU goals of these ventures are the production of water and/or its components from local resources. As a complement to the ESA 2025 mission, an instrument called ProSPA (PROSPECT Sample Processing and Analysis) is being developed at The Open University as part of ESA's Package for Resource Observation and in situ Prospecting for Exploration, Commercial Exploitation and Transportation (PROSPECT) (Barber et al., 2017) on-board the Luna-27 mission. As part of the Luna-27 mission, currently aimed for a launch in 2025, PROSPECT aims to identify and quantify volatiles at a high-latitude region of the Moon. The volatiles in question will be released by heating samples of regolith to temperatures of up to 1000 °C. In addition to determining the lunar volatile inventory, ProSPA will perform a proof-of-principle ISRU water/oxygen extraction experiment on the lunar surface.

Numerous methods have been hypothesized for extracting oxygen from the lunar regolith which fall into three main categories (Taylor & Carrier, 1993); solid/gas interaction, silicate/oxide melt, and pyrolysis. Each process has advantages and disadvantages with respect to the feedstock used, the resupply mass of any required materials (i.e. reactants or hardware), the complexity of the process, and the energy required. The titanium- and iron-bearing mineral ilmenite ($FeTiO_3$) is found in lunar basalts in varying concentrations (Papike et al., 1991), and has been proposed as a

potential source of oxygen (Taylor and Carrier, 1993). Reduction by hydrogen has long been considered the optimum method of extracting oxygen from ilmenite in lunar samples (Gibson & Knudsen, 1985). The main benefits being that hydrogen (of solar wind origin) can be extracted from the lunar regolith which reduces the resupply mass from Earth, its relatively low operating temperatures at 700-1000°C (Taylor & Carrier, 1993), and its simple operational process (Christiansen et al., 1988; Zhao & Shadman, 1993).

Reduction of ilmenite by hydrogen gas is an equilibrium reaction (1), with the physical state of each reactant and product denoted as (s) solid or (g) gas:

$$FeTiO_{3(s)} + H_{2(g)} \rightleftharpoons Fe_{(s)} + TiO_{2(s)} + H_2O_{(g)} \quad (1)$$

In order to maintain the reduction, the water vapor produced by the reaction needs to be constantly removed from the gas phase, e.g. via a flowing gas to a condenser. Taylor et al. (1993) suggested that the partial pressure of H_2O vapor at the reaction site must remain below 10 % for the reaction to continue, whilst work by Altenberg et al. (1993) suggested that up to 30 % partial pressure of H_2O is permissible for the reaction to continue when operating in low pressures of 1-100 mbar at 900 °C.

Previous studies, aimed specifically at ISRU capabilities, have used gas and/or vibrational fluidization techniques which improves mixing of the reactants and removal of the produced water (Christiansen et al., 1998; Gibson & Knudsen, 1985; Linne et al., 2009, 2012). A Significant limitation of the ProSPA system is that it is a static (non-flowing) and stationary (no fluidized bed or rotating drum) system, that utilizes a static volume of hydrogen gas. Instead, a cold trap is used to remove any water that is

produced, as suggested by Williams et al. (1979) and Williams & Mullins (1983), and maintains a sufficiently low level partial pressure of water at the reaction site.

The ProSPA system adopts heritage from Ptolemy (Wright et al., 2007) and the Gas Analysis Package, GAP (Talboys et al., 2009), and is primarily designed for the characterization of volatiles, and isotope analysis. ProSPA, therefore, did not originate with an ISRU focus and as a consequence has a non-ideal configuration for such experiments. The purpose of the present work is to investigate the feasibility of performing an ISRU demonstration with the ProSPA flight instrument on the lunar surface. The ProSPA analytical laboratory contains much of the requisite hardware – for instance furnaces capable of heating the sample to 1000 °C, hydrogen gas supply, a gas control system, pressure sensors, a cold finger for collecting volatiles, and two mass spectrometers to monitor the reaction (Barber et al., 2018). A static system simplifies the ProSPA design, avoiding the need for complex reactors, and gas circulation system. This work therefore concerns the evaluation of the feasibility of ProSPA to demonstrate hydrogen reduction of ilmenite grains to produce water in a static system.

Of the iron oxide bearing minerals available on the Moon, ilmenite will most readily reduce (Allen et al., 1994), and therefore produce the highest yields in a given time when reduced with hydrogen. Although ilmenite is thought to be found in relatively high concentrations of up to 20 % by volume in mare regions (Warner et al. 1978, Chambers et al. 1995, Papike et al. 1998, Hallis et al. 2014), highland regions, such as the high latitude regions where Luna-27 is expected to land, can contain <1 % by volume (Taylor et al., 2010). To avoid the possibility of little to no measurable yield, pure

ilmenite was chosen for this initial study to ensure the system is first capable of reducing the mineral. Lunar soil and simulants at this stage of the study would also complicate results as a consequence of their complex mineralogies which could cause secondary reactions to take place. As well as determining whether ProSPA can be used to perform ilmenite reduction reactions, this study aims to determine how the quantity of ilmenite present affects the measured yield. This will ultimately enable ProSPA to quantify the water that can be produced from ilmenite-bearing lunar soil.

2 Materials and Methods

2.1 System design

In terms of space instrument design, a so-called breadboard model is one that replicates the intended functionality without recourse to using highly specialized space-qualified components, and is largely free of the overall mass/volume/power consumption constraints imposed on flight hardware. One of the breadboard models of the ProSPA gas processing system, known as the Benchtop Demonstration Model (BDM) is shown in Fig. 1(a). The BDM is based on the overall ProSPA system diagram (Barber et al., 2017). A schematic diagram of the section of the BDM used for evaluating the ISRU experiment is shown in Fig. 1 (b)

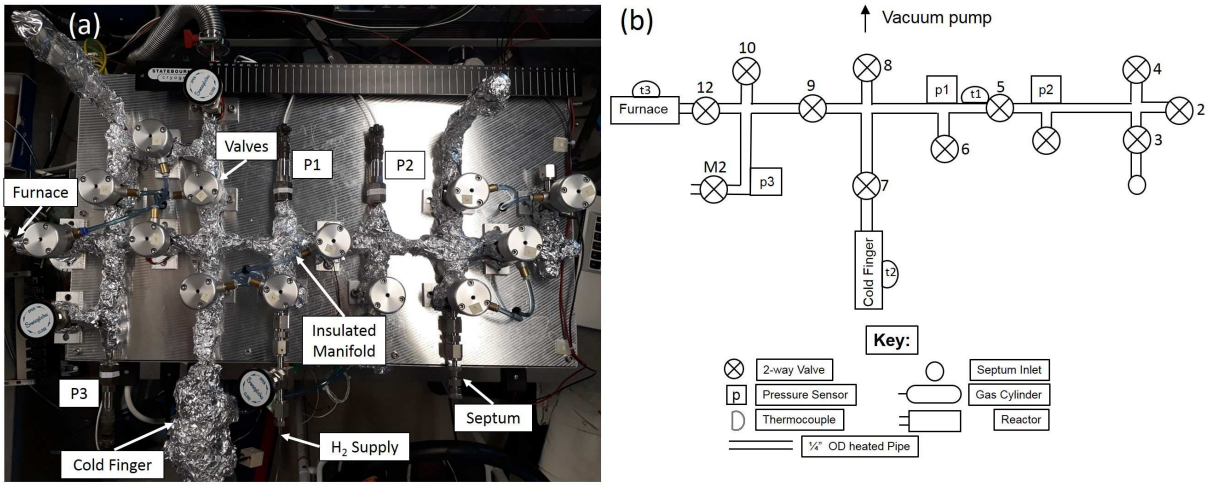

Fig. 1 (a) Labelled BDM image (b) BDM system diagram.

The purpose of the BDM is to be a testbed for ProSPA flight components and science experiments. The details of the BDM design are described in Supplementary Material (S1). It contains mainly commercial off the shelf parts connected together in a similar configuration to that of the intended flight design.

The sample 'oven' consists of a 200 mm long ceramic tube (LEWVAC, 99.7% Al2O3) of 4 mm internal diameter (ID) and 6 mm outer diameter (OD). It is placed inside a resistance-element furnace capable of reaching temperatures of 1200 °C (Fig. 2a). The ProSPA flight ovens (Fig. 2b) have internal dimensions of 4 mm ID and 13.6 mm depth and are designed to hold a sample mass of ~50 mg. As such the BDM oven arrangement replicates the flight oven's 4 mm internal diameter, ensuring the sample is held in the same shape as would be in the ProSPA oven. Although the hot zone is significantly greater in the BDM design, both the BDM and ProSPA oven hot zones are sufficient to uniformly heat a 50 mg ilmenite sample.

The BDM cold finger temperature was controlled by an automated supply of nitrogen gas cooled by passing through a liquid nitrogen dewar, in combination with an electric heating wire. Hydrogen gas (Laborgase, 99.999% purity) was supplied from a 12 L lecture bottle. The pressure of gas in the system was measured by silicon on insulator (SOI) diaphragm pressure sensors (Kulite, ETL-375CO-1.1BARA), and the manifold was heated by heater tape to 115 °C in order to prevent water vapor condensing when measuring vapor gas pressure. The valves and pressure sensors were not directly heated in order to avoid exceeding their permissible temperature range; they therefore operated at ~65 °C and 35 °C, respectively. Internal volumes of the BDM pipework were calibrated by expanding dry nitrogen gas from a 2 L volume incrementally into various sections of the extraction system. With the initial volume and pressure known, and with temperature remaining constant throughout the expansion, the change in pressure recorded during each expansion correlates to a change in volume.

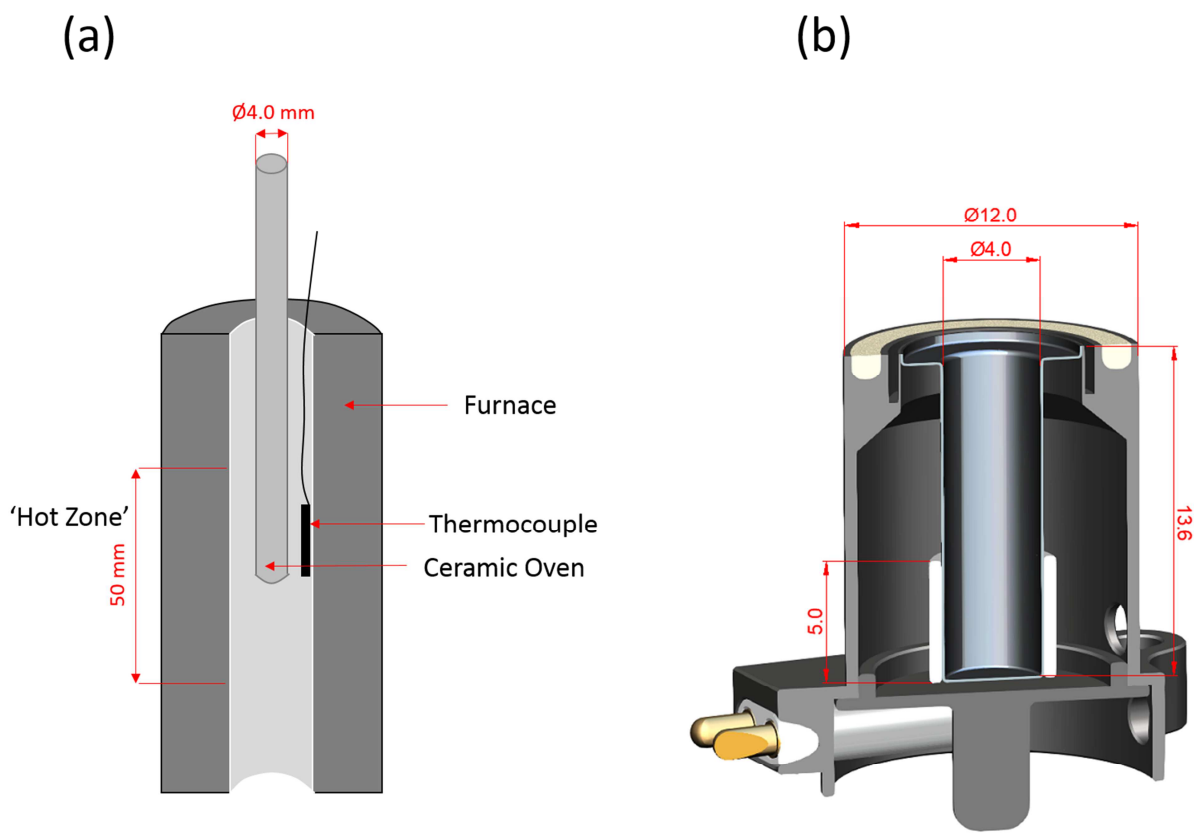

Fig. 2 (a) Furnace heater design, cross section. (b) ProSPA oven design CAD drawing. The samples are deposited by the drill into the 4 mm ID oven and heated by an electrical resistance element.

2.2 Ilmenite Feedstock

The ilmenite feedstock used in this work was supplied by the ESA European Astronaut Centre (EAC) in Cologne, Germany. According to mineral analyses by EAC, it is dominated by modal ilmenite (95 %) with some minor modal impurities comprising of silica (1-2 %), quartz (1-2 %), and other phases (1-2 %). A representative aliquot of ilmenite feedstock was used for grain-size distribution analyses using a Nikon SMZ1500 microscope and images taken with infinity capture software at a magnification of 10x before being analyzed in Image J open source software. Assuming that the grains are

spherical, the grain diameters were determined to be between 80 and 260 μm with an average diameter of 170 μm across the randomly selected grains analyzed. Although still relatively coarse compared to lunar soil, it was determined to be a suitable proxy for ilmenite that is found in lunar soils as for example in an Apollo 17 soil, ilmenite was found to have grain sizes of 45-500 μm (McKay et al., 1991). To remain representative of ProSPA capabilities, ilmenite samples of 45 mg (0.3 mmol) were used in the following ilmenite reduction studies.

2.3 Thermogravimetric – Mass Spectrometry (TG-MS) Analysis

TG-MS analyses were performed using a Netzsch Jupiter STA (Simultaneous Thermo-Analyzer) 449C, coupled to a Hiden HPR-20 quadrupole mass spectrometer via a stainless steel crimped capillary inlet.

To determine the temperature of bake-out, a 134.9 mg ilmenite sample was heated using a 3-stage ramp; from room temperature to 100 °C at 5 °C min^{-1}, followed by a 30 minute isothermal stage, heated at 2 °C min^{-1} from 100 °C to 520 °C, followed by a 60 minute isothermal stage and a final ramp at 5 °C min^{-1} to 660 °C followed by a 15 minute isothermal stage. At the time of analysis, 660°C was the highest possible temperature achievable by the TG-MS equipment. The consumption rate of gas from the simultaneous thermo-analyzer can be approximated to 16 cm^3min^{-1} helium. The mass spectrometer was operated in multiple ion detection (MID) mode, monitoring m/z 18 (H_2O^+), 28 (N_2^+, CO^+, including from CO_2 fragmentation), 32 (O_2^+), and 44 (CO_2^+). The resulting gas pressure profiles and the temperature profile are shown in Fig. 3(a) where a baseline corrected background reading has been subtracted from the data. As

a result of this data correction, the spectra is used for peak identification rather than a quantitative analysis. The major constituent of the released volatiles is water, with the initial release of atmospheric water on the surface of the grains coinciding with the start of the first temperature ramp and completing during the associated isothermal phase (at 100°C). A second m/z 18 release was observed during the next heating step, with the peak maximum at 450°C, likely a result of water release from hydrated mineral impurities. As the temperature was still increasing during this time, 450°C is easily higher than the temperature required to remove such water from the sample. A small m/z 44 peak is observed in line with this peak, suggesting decomposition of trace minerals has been observed. The following suppression of the signal at m/z 44 is then observed, but this corresponds to a minor artefact in the blank values used to correct this data and is likely not a true feature. As this is a comparatively limited release of material over an extended time, these features are relatively small and the m/z 28 peak that would be expected, corresponding to the m/z 44 peak for CO_2, is not clearly observed. The m/z 28 and 32 spectra indicate no clear peaks suggesting they represent background levels of N_2 and O_2. As a result of this study, a bake-out temperature of 500 °C was chosen for the following ilmenite experiments. This was expected to remove all water present from the ilmenite sample before the hydrogen reduction reactions were performed. This would enable a more accurate quantification of the calculated yield of oxygen and reduction extent during the ilmenite reduction studies.

The bake-out time required was determined by heating a 110.0 mg sample of ilmenite to 500°C at 40°C min^{-1} and following this with a 1.5 hour isotherm. The results (background corrected for blank sample) are shown in Fig. 3 (b). There is a rapid

233 release of volatiles, and therefore higher pressures measured in this experiment
234 compared to the previous slower temperature ramp experiment. Using this increased
235 heating rate, a sharp m/z 18 peak was observed, with the release appearing completed
236 before the isothermal stage, the signal then stabilized as the gases sampled from the
237 thermo-analyzer reached equilibrium at the higher temperature. A small peak at m/z 44
238 (CO_2^+), and corresponding m/z 28 peak ($N2^+$, CO^+ from fragmentation of CO_2) were
239 observed in line with the m/z 18 peak as adsorbed moisture from the air is released. As
240 the purpose of this analysis was primarily to identify water release, no specific cleaning
241 or drying methods which could potentially affect moisture content were applied to the
242 sample before analysis. These analyses do not, therefore, attempt to distinguish if these
243 releases are part of the sample or foreign matter. Background levels within the system
244 appear to have fully equilibrated by 4000 s, representing approximately 50 minutes into
245 the isothermal stage. Total mass loss was approximately 0.35 % of the starting sample
246 mass (385 µg). From this analysis a bake-out time for the ilmenite samples of 1 hour
247 was selected.
248

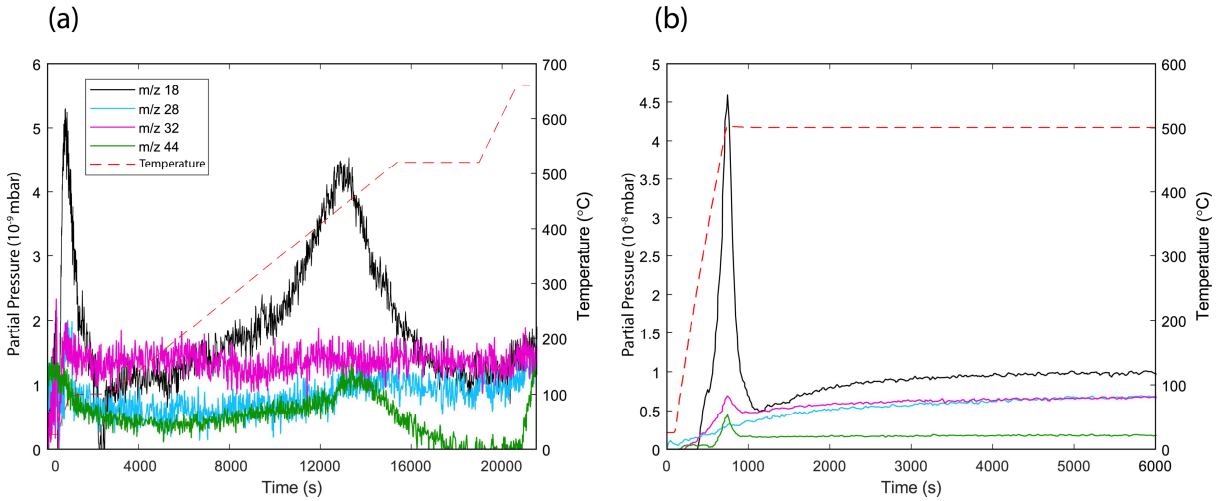

249
250 *Fig. 3 (a) The gas release profile for ilmenite when heated up to 660 °C with a variable*

heating ramp. (b) The gas release profile for ilmenite when heated at a rate of 40 °C min^{-1} up to 500 °C followed by a 1-hour isotherm.

2.4 Water calibration

In this work the quantity of water produced from the reduction of ilmenite is estimated by measuring the pressure of the water in a sealed system. However, water is susceptible to 'sticking' to cold spots in the system, where the strong polarity of water molecules leads to greater adsorption of water onto surfaces (Pfeiffer Vacuum, 2013). Typically, vacuum systems that process water samples are maintained at temperatures of ~100 °C but to account for the relatively high volumes of water anticipated in the system, the manifold was kept at 115 °C to aim to keep water in the vapor phase. However, with the need for specific components to operate at cooler temperatures (e.g. valves and pressure sensors) it was necessary to characterize the behavior of water vapor in the BDM. A calibration study was performed and is detailed in Supplementary Material (S2). The results from the study showed that for measured pressures, P_m, of water < 120 mbar, the equivalent pressure of water when assuming an ideal gas, P_i, can be calculated as $P_i = F \times P_m$. Where F is a calibration factor defined as follows:

$$F = 3.76 \times 10^{-5} \times {P_m}^2 + 8.79 \times 10^{-4} \times P_m + 1.00 \qquad (2)$$

At low pressures F approaches 1, with F = 1.03 at 20 mbar. This calibration factor can be applied to determine the pressure that would be observed if water produced from ilmenite reduction experiments behaved as an ideal gas and not condensing at cold spots. This ideal pressure is used to calculate the yield of oxygen as a result of the reactions.

2.5 Ilmenite reduction experiment parameters

For the following experiments the bake-out temperature of 500 °C and duration of 1 hour had been determined by the TG-MS analysis (section 2.3). A range of ilmenite masses, 11.2 mg, 23.0 mg, 33.7 mg, and 44.7 mg were reacted, and the quantity of hydrogen was chosen for all reactions as 0.30±0.01 mmol, sufficient to achieve complete reaction of a 45 mg ilmenite sample (0.3 mmol) according to Eqn. (1). Higher pressures of hydrogen could increase the extent of water production by maintaining a water concentration of <10 %, however, the high pressure may also reduce the rate of diffusion of water away from the reaction site (and thereby smother the reaction). A manifold temperature of ~115 °C was chosen to aim to keep water in the vapor phase (see section 2.4). A reaction temperature of 900 °C was chosen as a suitable starting point for ilmenite reduction studies as it is the minimum temperature required to obtain reasonable reaction rates (Christiansen et al., 1988) and is within the operating range of ProSPA. A reaction time of 1 hour was selected as this is within the ProSPA operational power and time requirements.

2.6 Ilmenite reduction experimental procedure

To determine if ilmenite can produce water in a static system, different quantities of ilmenite were heated in the presence of hydrogen. Any water produced as a result of this reaction, was condensed at the cold finger (see Fig 1b). After the duration of the experiment the cold finger was then heated to release the water which was measured via a pressure sensor. Ilmenite is reacted in these studies to quantify the water that can be produced from the reduction of the iron oxide bearing mineral. Although the ilmenite

used in this work contains 5% other mineral traces, the effects on the reaction of such impurities are assumed to be minimal. The interfering factors arising from the inclusion of other lunar minerals will be investigated in future work with lunar simulants and samples. The steps for each ilmenite reduction reaction were:

Sample Loading: The weighed sample was loaded into the ceramic oven and attached to the BDM and evacuated to a pressure $<10^{-6}$ mbar as measured at the vacuum pump.

Bake-out: The oven was heated to a bake-out temperature of 500 °C for 1 hour to remove any volatiles and the pressure of released volatiles was measured. After the bake-out, the volatiles were evacuated through vacuum pumps via valve 8.

Hydrogen Addition: ~ 0.3 mmol of hydrogen gas was introduced into the BDM

Reaction: The cold finger was cooled to -180 °C and the oven was heated to the reaction temperature of 900 °C. During the 1 hour reaction the residual pressure of hydrogen was measured continuously by monitoring the gauge p1.

Non-Condensable Removal: The hydrogen (and any non-condensable volatiles) were removed by pumping to vacuum, as measured at the vacuum pump.

Water Release: The cold finger was heated to 115 °C at a rate of ~125 °C min^{-1} and the amount of water produced measured on gauge p1.

318 Post reaction: Once the oven had cooled to room temperature, grains were
319 removed from the oven and prepared for Scanning Electron
320 Microscope (SEM) analysis.

321 An outline of the experimental procedure is shown in Fig. 4. It should be noted that the
322 assumed average system temperature used for analysis is taken to be 115 °C. Although
323 valves and pressure sensors may be operating at lower temperatures, they represent
324 relatively small volumes of the entire system.

325

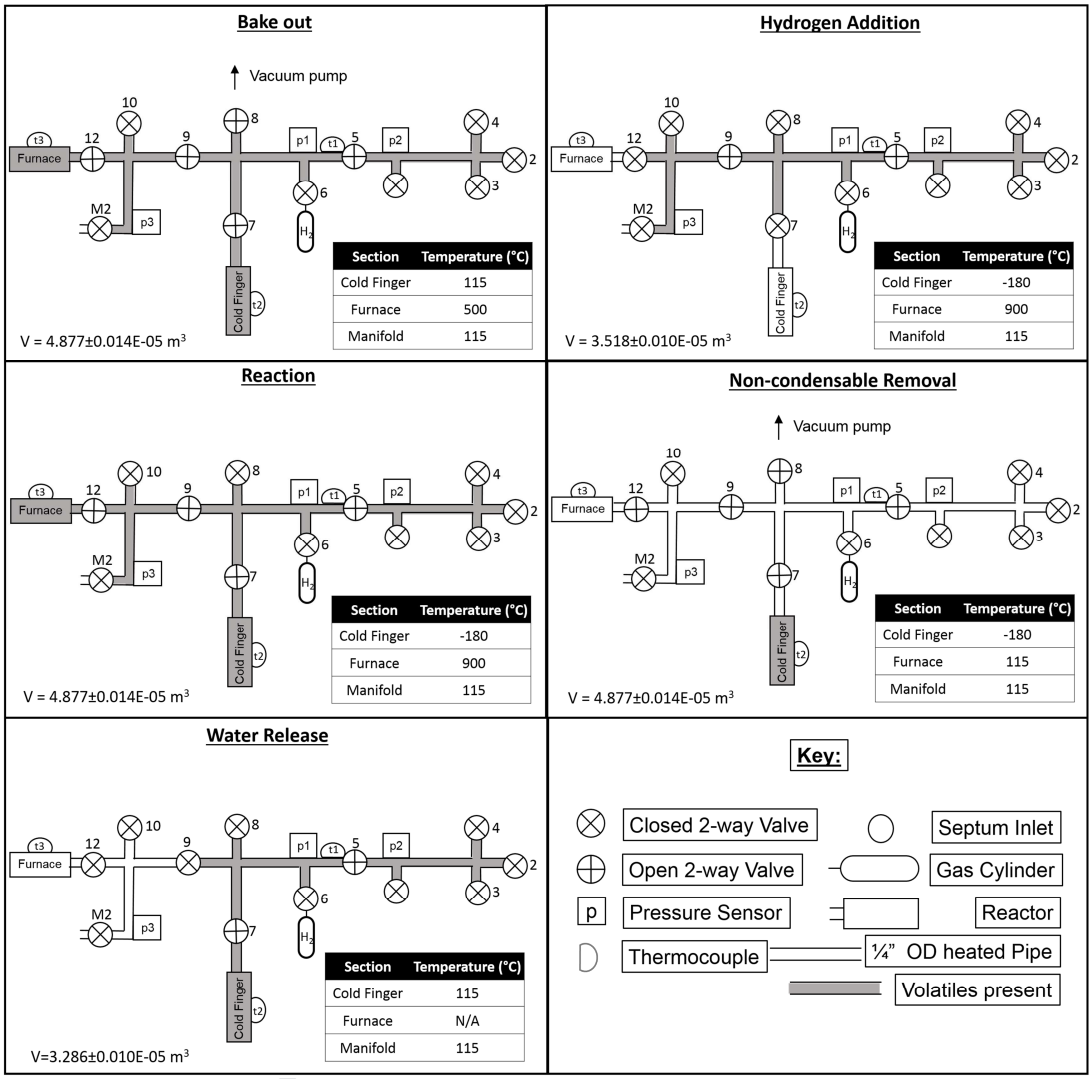

Fig. 4 Volumes and temperatures for each phase of the ilmenite reduction study, where the cold finger, furnace, and manifold are separately thermally controlled.

After each experiment, ilmenite grains were analyzed for evidence of the reduction reaction. A random selection of grains from each reacted sample, and an unreacted sample were set in epoxy resin in 10 mm brass rings and then polished and carbon-coated for analysis using a FEI Quanta 200 3D FIB-SEM.

3 Gas Transport Analysis

To determine the extent to which ilmenite reduction reactions are feasible with ProSPA, two models were used to identify the time scales involved for the produced water to diffuse through the system. The gas flow type and consequently the diffusion rate are discussed. The flow of molecules in a vacuum system can be characterized as either viscous, transitional, or molecular flow. Once the type of flow has been established, it is possible to estimate the time taken for the water molecules produced in the reaction to be replaced by hydrogen molecules, and for the reaction to continue. The Knudsen number, K_n, is used to characterize the flow of gas within a system as follows (Delchar, 1993):

$$Viscous\ flow \quad K_n < 0.01$$

$$Transitional\ flow \quad 0.01 \leq K_n \leq 1$$

$$Molecular\ flow \quad K_n > 1$$

The Knudsen number for the flow of water from the furnace to the cold finger in the ProSPA system was estimated for a simplified pipe of length *l*, radius r, and uniform temperature, *T*, where the volume of the pipe, *V*, is defined as $V=l\pi r^2$.

Eqn. (3) is used to calculate the Knudsen number for a system where λ is the mean free path of a gas particle and *a* is the radius of the pipe.

$$K_n = \frac{\lambda}{a} \qquad (3)$$

The calculations and data used to determine the mean free path of gas molecules expected in the system is outlined in more detail in Supplementary Material (S3). A trapping efficiency ϵ is considered which determines how much of the produced water is

353 condensed at the cold finger, where a value of 1 means 100% of the water is
354 condensed.

355

356 The Knudsen number was determined for the ilmenite concentrations trialled in
357 this work, 25%, 50%, 75% and 100% of the 45 mg standard mass. A pipe of length 1 m
358 and internal diameter of 4 mm is assumed. As the trapping efficiency is unknown, a
359 trapping efficiency of 0.5 and 1 are shown in Fig. 5.

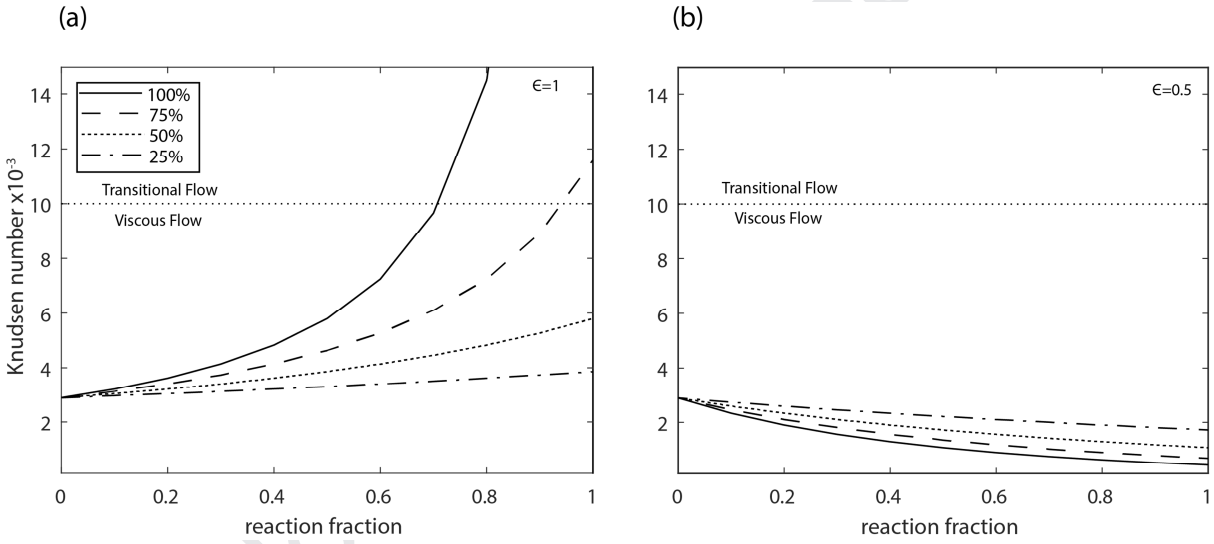

360

361 *Fig. 5 Knudsen number for a range of ilmenite concentrations throughout the reduction*
362 *reaction considering a trapping efficiency of (a) ϵ = 1, and (b) ϵ = 0.5.*

363 When it is assumed that all the water produced is immediately condensed (ϵ=1), the
364 Knudsen number increases as a result of the lower pressure in the system. However,
365 when only 50 % of the water produced is condensed (ϵ=0.5), the relative proportions of
366 water molecules to hydrogen molecules increases, which leads to an increase in the
367 average diameter of molecules in the system with time and the gas flow becomes more
368 viscous. It is assumed that the gas flow will be mostly viscous and so water must first

diffuse through the hydrogen gas before collecting at the cold finger. To estimate the diffusion rate of water from the reactor to the cold finger, a simple model was considered with a partial pressure of 10 % water vapor at the furnace and 0% water vapor at the cold finger. A partial pressure of 10 % was chosen as a boundary condition in line with the assumptions contained within Taylor et al., 1993).

The diffusion rate can be derived from the molar flux of water (gas A) into hydrogen (gas B) using Eqn. (4), which is adapted from Fick's law in Geankoplis (1993).

$$J_{AZ} = D_{AB} \frac{(P_{A1} - P_{A2})}{RT(Z_2 - Z_1)} \quad (4)$$

J_{AZ} is the molar flux of gas A, D_{AB} is the diffusion coefficient which defines the molecular diffusivity of gas A in gas B, R is the molar gas constant, T is the average temperature of the system (K), and $z_2 - z_1$ is the distance of diffusion. P_{A1} and P_{A2} are the pressures of gas A within the furnace volume and at the cold finger respectively, assuming P_{A2} is 0 Pa for a first order approximation. P_{A1} is derived from the ideal gas law using the pipe volume, V, the pipe temperature, T, and the total number of moles of water produced presumed to be at the start of the pipe, n_A. n_A is defined as 10% of the moles of hydrogen in the system, n_B.

The molar flux of water into hydrogen can be used to determine the time of diffusion, t, across the length of the pipe using the concentration of water molecules in the pipe, C_A as in Eqn. (5):

$$t = \frac{l \cdot C_A}{J_{AZ}} \quad (5)$$

The calculations and data used to determine the diffusion time in the system are outlined in more detail in S4.

With 0.3 mmol of H_2 (translating to a system pressure of ~198 mbar) and a partial pressure limit of 10% of water at the furnace, the calculated diffusion time is ~170 s (1.8 μmol s^{-1}. Providing the diffusion of water vapor away from the reaction site is the rate controlling step, this suggests that all the water that can be produced from the reduction of 45 mg of ilmenite can be collected on the time scale of a few hours and therefore be feasible within the ProSPA system. There are limitations to these models but they provide a good first order analysis of the feasibility of the reaction.

3 4Results

The reaction and water release phases of each individual ilmenite reduction experiment are considered below in detail.

4.1 Ilmenite reduction: Reaction Phase

Following bake-out, the ilmenite is reacted for 1 hour with 0.3 mmol of hydrogen at 900 °C. The pressure profiles during the reaction of each sample is shown in Fig. 6. The hydrogen present in the system should react with the ilmenite to produce water in an equal number of moles (1), which in itself should result in no net change in the pressure of the system. However, with the cold finger operating at -180 °C, this water is condensed at the cold finger removing water from the gaseous phase and reducing the pressure in the system. Therefore, a pressure drop is recorded, corresponding to the conversion of H_2 to H_2O and the subsequent removal of gaseous H_2O by the cold trap. An estimated quantity of H_2 in moles, n_h, that has reacted is also shown in Fig. 6, calculated from the ideal gas equation where*:*

$$n_{h|w} = \frac{p \times V}{R \times T} \qquad (6)$$

Where p is the pressure in the system with an uncertainty of ±1 mbar, the volume of the system V is taken from Fig. 4, R is the ideal gas constant, and the assumed temperature of the system T is at 115 °C (388 K).

The initial and final pressure in the system is recorded in Table 1 for each sample, along with the calculated amount of hydrogen that has reacted. It can be assumed that during the reaction the gases were moving in the viscous flow regime as pressures of > 105 mbar were recorded (Pfeiffer Vacuum, 2013).

The results show that with increasing ilmenite mass the pressure change increases, showing that more hydrogen has been converted to water. The pressure is still dropping after 60 minutes indicating the reaction has not neared completion in this time.

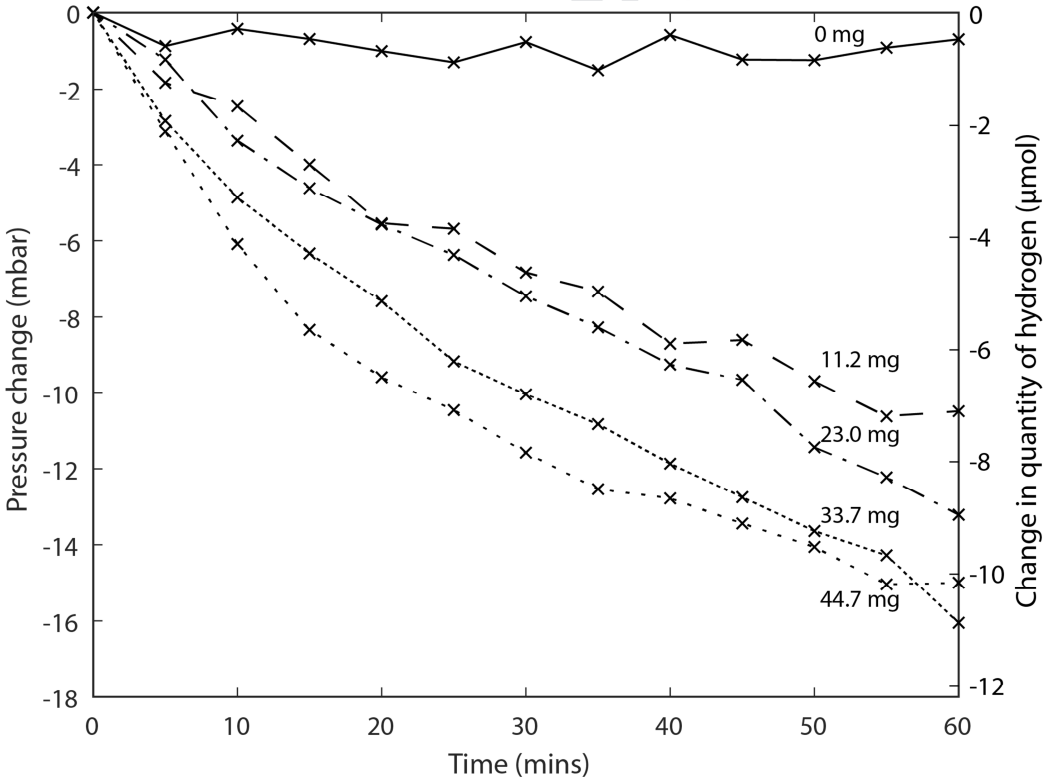

Fig. 6 Pressure change and equivalent change in amount of hydrogen with time during the reaction phase with varying masses of ilmenite.

4.2 Ilmenite reduction: Water release phase

The final phase of the experiment, the water release stage, is where the cold finger is heated to 115 °C and the pressure in the system is recorded for 1 hour. As the cold finger is heated quickly (~125 °C min^{-1}) from -180 °C to 115 °C, there is a small peak at ~5 minutes where water is likely released and re-condensed on a cold spot as a result of non-uniform heating of the cold finger. It takes a further ~10 minutes for the pressure in the system to start to rapidly increase as condensed volatiles are re-released as gases into the system (Fig. 7a). The initial pressure rise is then followed by a downward drift in pressure. With increasing ilmenite mass, the peak pressure increases because of more volatiles being released. For higher ilmenite masses, the pressure profiles are limited to ~16 mbar. It is assumed that the pressure rise during the water release stage is wholly as a result of water vapor produced from the ilmenite reduction reaction. The equivalent production of water n_w from each ilmenite sample is calculated using Eqn. (6), by assuming the associated pressure rise is a result of the production of water only, and included in Fig. 7(a). The amount of hydrogen reacted to produce water from the reaction phase is compared to the amount of water produced from the water release phase and shown in Fig. 7(b). Uncertainties are calculated using the propagation of uncertainties from the manifold temperature (±5°C), volume (Fig. 4), and pressure values (±1 mbar). The temperature uncertainty is derived from the variation in manifold temperature, the volume uncertainty is derived from the standard deviation in volume calculations performed from the expansion of gases in the system, and the pressure uncertainty is derived from the uncertainty of the sensor. The reaction phase data suggests that more hydrogen is reacted (and therefore water produced)

than compared to the water release data. One cause for this discrepancy would be inefficient trapping of water at the cold finger, perhaps water sticking in the system before reaching the cold finger. All pressure and equivalent water quantity data are shown in Table 1, along with a calibrated pressure value as determined using Eqn. (2).

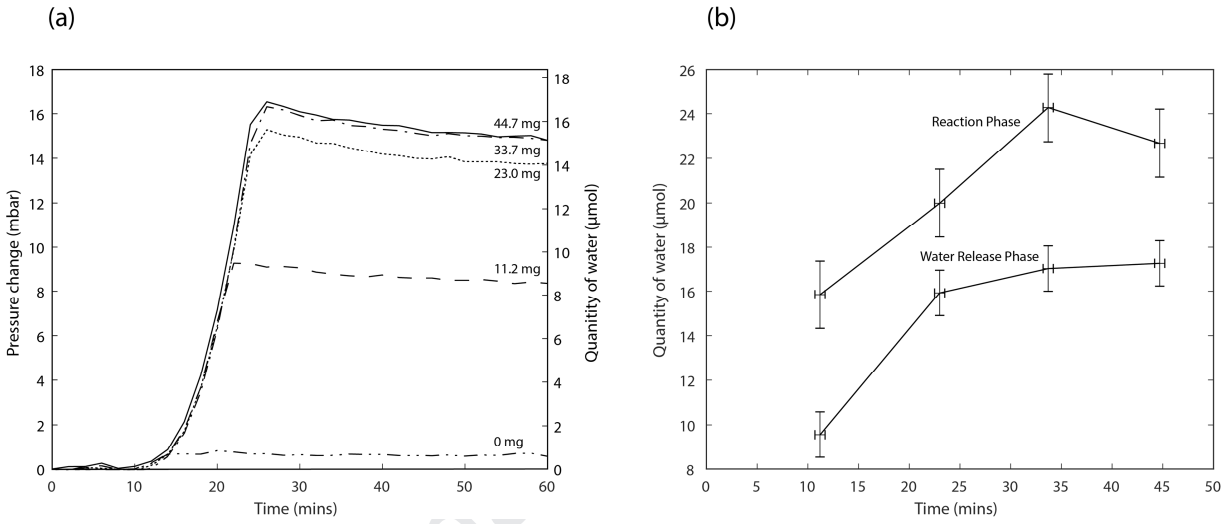

Fig, 7(a) Pressure rise and equivalent water production with time during the water release phase with varying masses of ilmenite. (b) Estimated water produced from varying ilmenite masses as calculated from pressure data during the reaction and water release phases with a 1σ uncertainty.

4.3 Calculation of the reaction yield and efficiency

Although water is the product of the reduction reaction, its constituent oxygen is the resource most commonly referenced when discussing yields. There are many ways in which “yield” can be calculated. For instance, yield could be the mass of oxygen extracted compared to the sample mass, or the mass of oxygen extracted compared to the total oxygen in the sample, or the mass of oxygen extracted compared to the

maximum amount of oxygen that can be extracted (Eqn. 1). In addition, the yield can be calculated as the mass of water extracted.

Here "yield" is defined as the wt. % of oxygen extracted compared to the total sample mass, from here described as calculated oxygen yield (7). This term is more useful for ISRU and a mining perspective as the desired product is commonly oxygen and in this case it indicates the total mass of ilmenite that needs to be present in the regolith to obtain a certain quantity of oxygen. The calculated oxygen yield is the ratio between the mass of oxygen produced, m_o, with respect to the mass of ilmenite started with, m_{ilm}, The mass of oxygen produced can be calculated from the mass of water produced, m_w, by multiplying it by the ratio between the molar mass of oxygen, M_o, and the molar mass of water, M_w. The amount of water produced, n_w, can be substituted for m_w/M_w and can be calculated with Eqn. 7 and the pressure rise from the water release phase. In theory the maximum yield of oxygen from water for the ilmenite reduction process as given in Eqn. (1) is 10.5 wt. % oxygen.

$$yield = \frac{m_o}{m_{ilm}} = \frac{m_w M_o}{m_{ilm} M_w} = \frac{n_w M_o}{m_{ilm}} \quad (7)$$

When comparing the efficiency of a particular reaction it is more useful to measure the extent of the reduction reaction, ξ, derived from the ratio of the mass of oxygen produced, m_o, with respect to the maximum potential oxygen produced, $m_{o,max}$. The reduction extent is therefore equivalent to the amount of water produced as a percentage of the total water that could be produced by the reaction (Eqn. 8).

$$\xi = \frac{m_o}{m_{o,max}} = \frac{m_o M_{ilm}}{M_o m_{ilm}} \quad (8)$$

The yield outputs are summarized in Table 1 and Fig. 8, where the uncertainties are derived as in Fig. 7b. Maximum yield and reduction extent occurs in smaller masses of ilmenite. For a mass of 11.2 mg, peak oxygen yields of 2.3±0.2 wt. % and 1.4±0.2 wt. % are calculated for the reaction phase and water release phase respectively, equating to reduction extents of 21.5±2.3 % and 12.9±1.5 % respectively.

			Ilmenite mass (mg)				
			0	**11.2± 0.5**	**23.0± 0.5**	**33.7±0.5**	**44.7±0.5**
Reaction phase	Hydrogen pressure (mbar)	Initial	170.3± 1.0	171.0± 1.0	163.7± 1.0	168.9± 1.0	167.3± 1.0
		Final	169.6± 1.0	160.5± 1.0	150.5± 1.0	152.8± 1.0	152.3± 1.0
		Difference	0.7± 1.0	10.5± 1.0	13.2± 1.0	16.0± 1.0	15.0± 1.0
	Calculated hydrogen reacted (μmol)		1.0± 1.5	15.8± 1.5	20.0± 1.5	24.3± 1.5	22.7± 1.5
	Oxygen yield (wt. %)		n/a	2.3±0.2	1.4±0.1	1.2±0.1	0.8±0.1
	Reduction extent (%)		n/a	21.5±2.3	13.2±1.0	10.9±0.7	7.7±0.5
Water release phase	Pressure rise (mbar)	Measured	0.8± 1.0	9.3± 1.0	15.3± 1.0	16.3± 1.0	16.5± 1.0
		Calibrated	0.8± 1.0	9.4± 1.0	15.5± 1.0	16.6± 1.0	16.8± 1.0
	Calculated water produced (μmol)		0.8±1.0	9.5±1.0	15.8±1.0	16.9±1.0	17.1±1.0
	Oxygen yield (wt. %)		n/a	1.4±0.1	1.1±0.1	0.8±0.1	0.6±0.1
	Reduction extent (%)		n/a	12.9±1.5	10.4±0.7	7.6±0.5	5.8±0.4

Table 1. Details of the results for each ilmenite sample during the reaction phase and water release phase. Included are the pressure changes recorded, the calculated

amount of hydrogen used in the reaction, and the calculated amount of water produced. Oxygen yield and reduction extent are also included.

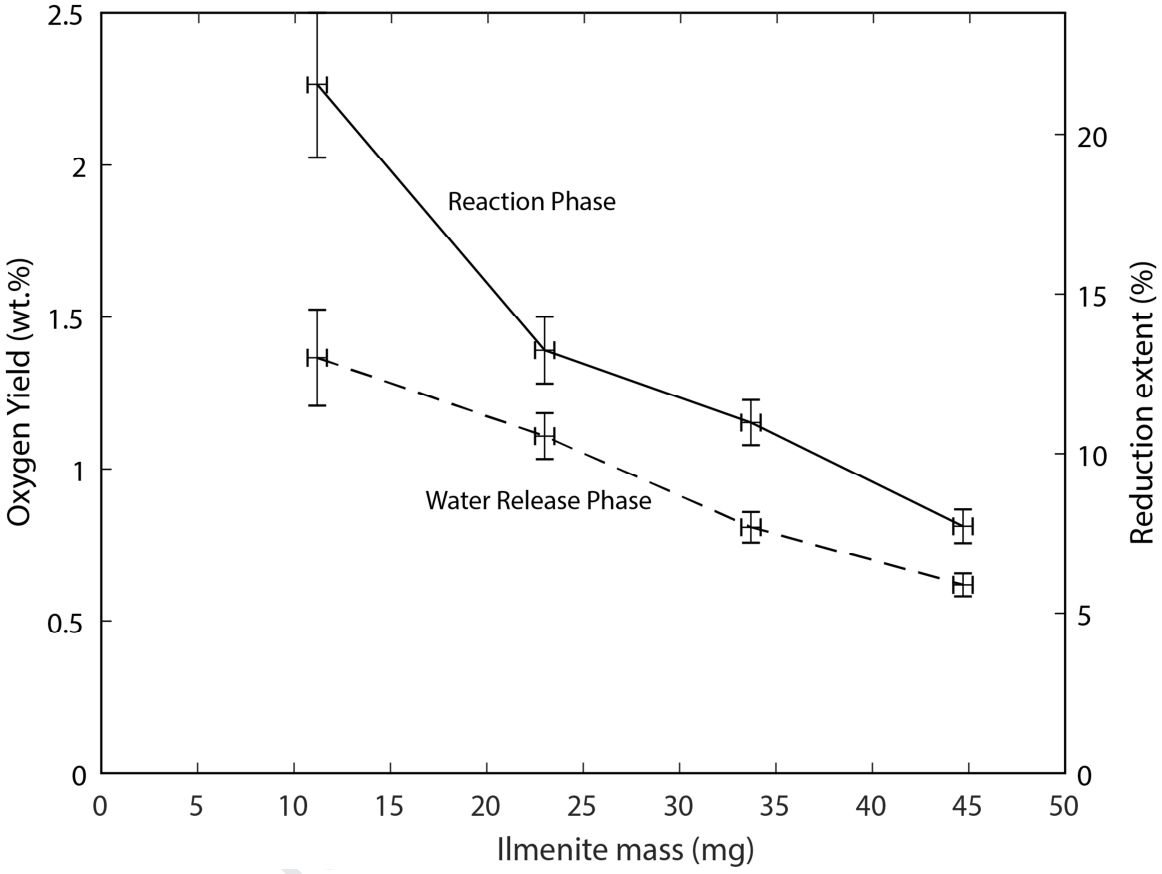

Fig. 8 Calculated yield and reduction extent derived from the reaction phase and from the water release phase with a 1σ uncertainty.

Section 4.4 Ilmenite grain analysis

The process of ilmenite reduction can be described by a shrinking core model as shown in Fig. 9 by Dang et al. (2015). The reaction of ilmenite proceeds from the surface to the interior of the grain as hydrogen diffuses inwards, reduces the ilmenite, and water diffuses out of the grain. Metallic iron forms on the outer edges of the grains

where the reaction has occurred, acting as a nuclei for further metallic iron formation towards the center of the grains. The shrinking core model suggests that reduction would occur quickly at first, as a larger surface area of ilmenite is exposed to hydrogen. As the reaction progresses the reduction process slows as the surface area decreases; in addition, hydrogen gas must diffuse through the reacted layer to access unreacted ilmenite and water needs to diffuse through the reacted layer to be removed. Zhao & Shadman (1993) discuss three stages of the reduction process; namely induction, acceleration and deceleration. The induction stage, a result of initially slow transport of iron from the ilmenite pores, is followed by an accelerated reaction rate until the ilmenite supply decreases to a point where the reaction is decelerated.

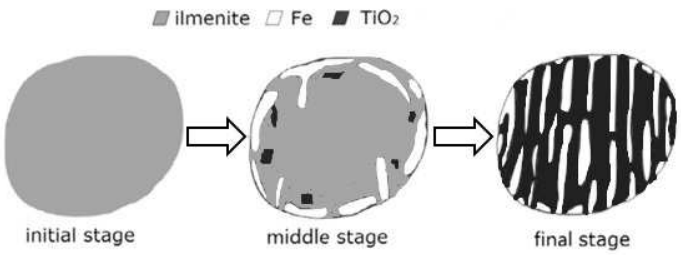

Fig. 9 Ilmenite grain reduction by hydrogen via the shrinking core model, adapted from Dang et al. (2015).

Approximately 15 mg of unreacted ilmenite grains were studied by Back Scatter Electron (BSE) imaging using a SEM (Fig. 10 a-d) where the contrast in gray-scale highlights differences in the average atomic numbers of constituent elements (Goldstein et al. 2017). Heavy elements such as Fe appear brighter as a result of a stronger backscatter of electrons. Some grains appear to have non-uniform chemical composition. They display lamellar features (likely rutile) corresponding to darker BSE

526 regions. An X-ray multi-element map of an unreacted grain (Fig. 10 e) shows relatively
527 homogeneous distribution of Fe and Ti contents with some Ti hotspots.

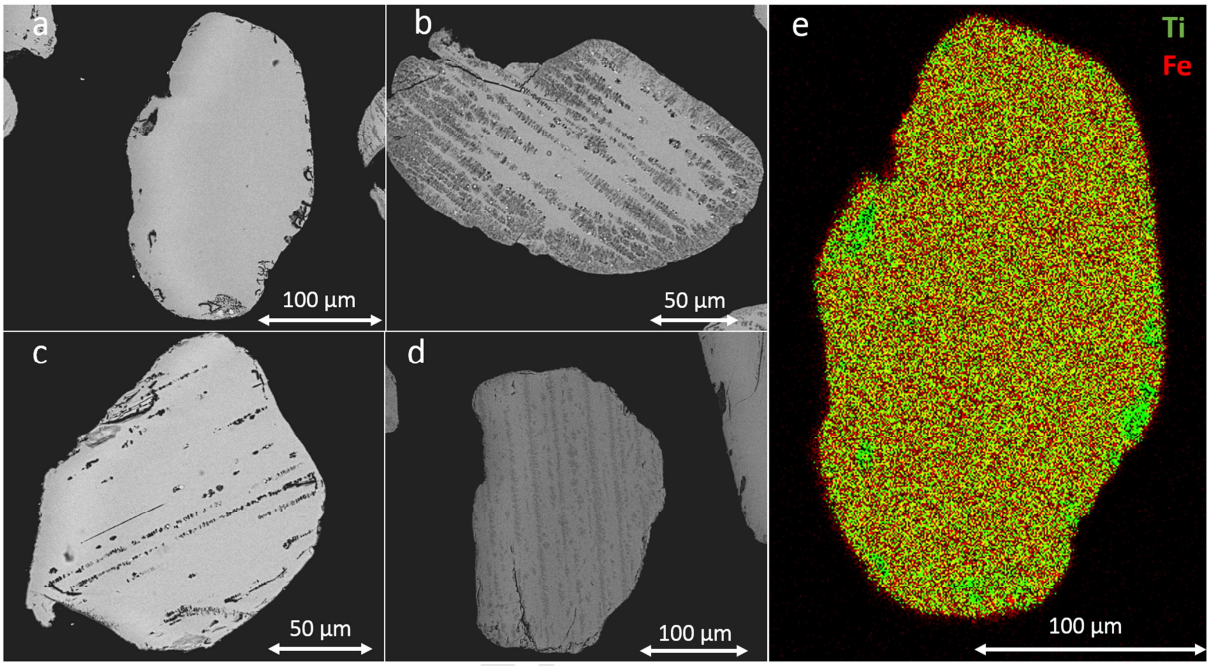

528

529 *Fig. 10 (a-d) Example BSE images of unreacted ilmenite grains. (e) Ti and Fe element*
530 *map of grain a.*

531 The reacted ilmenite samples were also analyzed using BSE. Approximately 15
532 mg was used for analysis from each sample, where the grains represent a random
533 selection from across the sample, and where the placement of the grains in the reaction
534 tube is not known. The reaction proceeded different amounts in different grains, likely a
535 result of their location within the tube. The reacted grains show further darkening in
536 terms of their BSE response and the production of bright spots (Fig. 11 a-d). There is
537 also a darkening and formation of bright spots on the edge of the grains. The darker
538 areas have a higher proportion of titanium whilst the brighter spots show an increase in
539 iron. It is likely that the lamellae can provide a pathway for hydrogen into the ilmenite

structure as they are a physically separate mineral structure within the main mineral structure. A reaction front can be seen moving inwards from the surface and producing metallic iron. This suggests that the reduction reaction occurs preferentially from the outside in, as shown by Dang et al. (2015), and along the lamellae supporting the shrinking core model (Fig. 9). An element map of one of the reacted grains (Fig. 11 e) show areas of concentrated Ti and depleted Fe, suggesting that Fe has been separated from the ilmenite leaving a TiO_2 residue. This trend follows the grain from the outside in, representing the extent to which the reaction has penetrated into the grain.

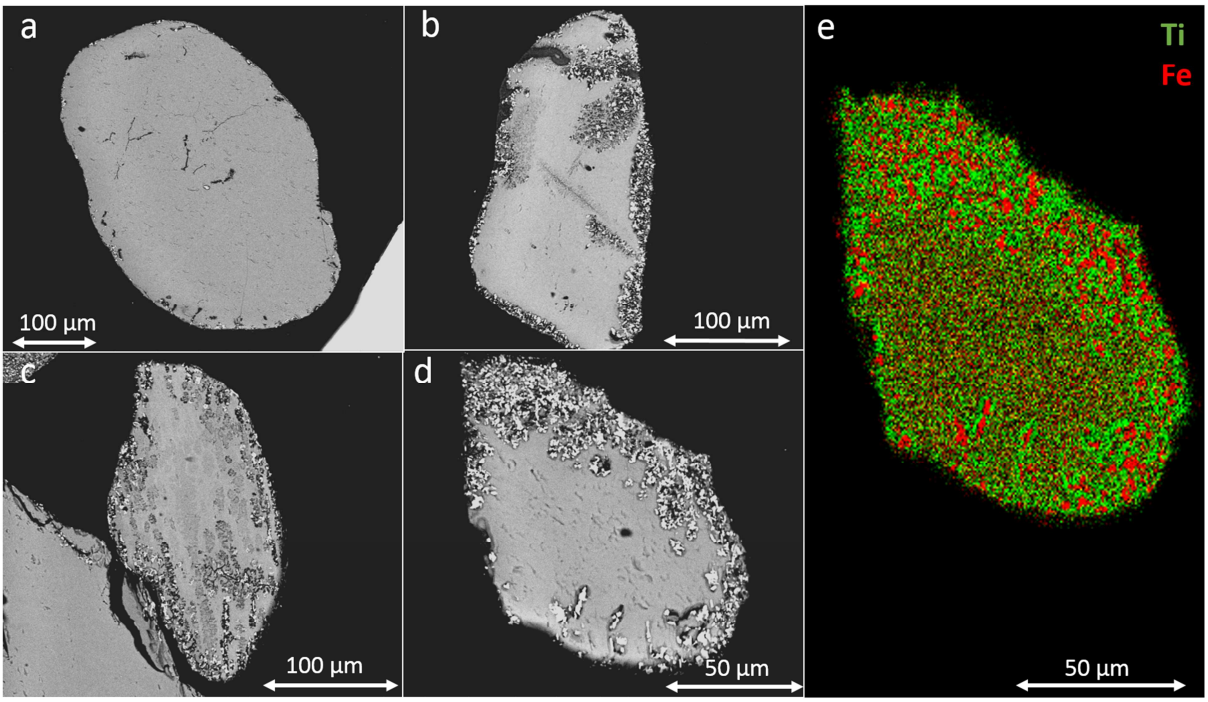

Fig. 11 (a-d) Example BSE images of reacted ilmenite grains taken from the 23.0 mg ilmenite sample. (e) Ti and Fe element map of grain d.

Each reacted sample was imaged using BSE. At a 500x zoom, two images were taken of random groups of grains for each reacted sample. The reduction extent was

553 determined using a scale from 0-4 (Fig. 12). The fraction of grains assigned to each
554 classification was then compared for each sample (Fig. 13). The fraction of grains for
555 each sample represent ~7%, 3%, 3%, and 2% of the 11.2 mg, 23.0 mg, 33.7 mg, and
556 44.7 mg sample respectively. As the grains imaged are from a random selection from
557 each sample, it is assumed that each analyzed image is representative of the entire
558 bulk sample.

559

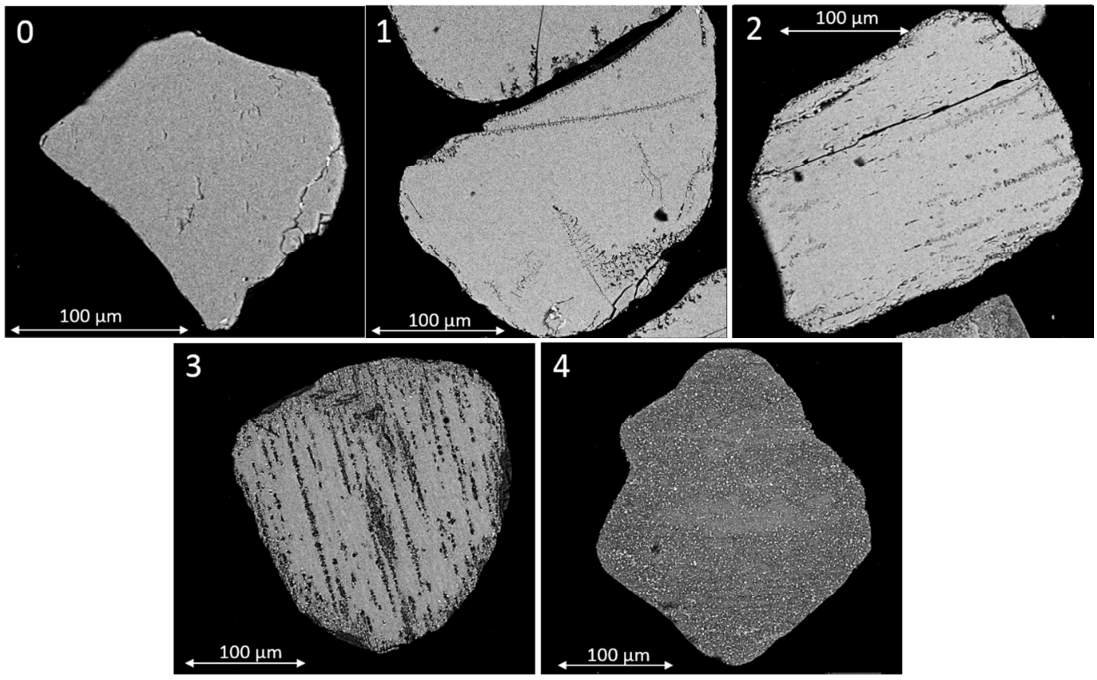

560

561 *Fig. 12 Reduction extent scale where 0 shows no reaction, 1 shows partial reaction of*
562 *the outer rim of the grain, 2 shows full reaction on the outer rim of the grain, 3 shows*
563 *significant penetration of reaction into the grain, and 4 shows complete reaction of the*
564 *grain.*

565

566

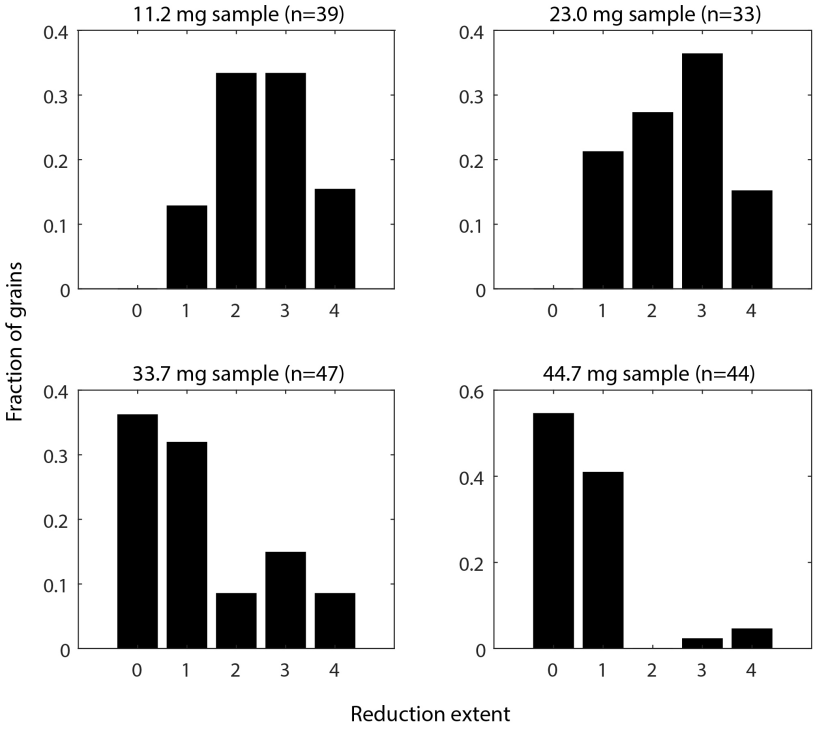

567

568 *Fig. 13 Histograms displaying the distribution of reduction extent, as defined by the*
569 *extent of the reduction reaction around and into the grain, as a fraction of the number of*
570 *grains for each sample size*

571 **5 Discussion**

572 The bake-out process was demonstrated to successfully remove volatiles from
573 ilmenite samples (See Supplementary material S.5). As a result, any volatiles measured
574 during the reaction and water release phases are likely only associated with the ilmenite
575 reduction process. It is therefore recommended that when ilmenite reduction is
576 performed on the lunar surface within ProSPA, a bake-out process be incorporated into
577 the extraction of trapped water ice and/or solar wind implanted particles (SWIP) from
578 the lunar regolith, and the volatiles would be analyzed and stored.

The reaction stage showed a greater hydrogen pressure drop in the system for larger samples (15.0 mbar pressure drop for 44.7 mg ilmenite) compared to the smaller samples (10.5 mbar pressure drop for 11.2 mg ilmenite) suggesting that more ilmenite has reduced to produce water which is then condensed. There is only one data set per sample mass available, however they appear to follow a predictable trend. As the pressure continues to drop for the entire 1 hour reaction time, it is assumed that the reaction has not reached completion. As the amount of H2 present in each study (0.3 mmol) is stoichiometrically sufficient to reduce a 45 mg (0.3 mmol) ilmenite sample, the smaller ilmenite samples will have an excess of hydrogen. The quantity of hydrogen was kept consistent so that the reaction pressures were consistent between experiments. It is assumed that only when the reactions are near completion will having an excess of hydrogen be relevant to the reaction rates. This would be confirmed with longer experiments. With the current setup and assuming as a first order analysis that the reaction rate is linear, it would take over 12 hours for the 45 mg ilmenite sample to completely reduce. This is not suitable for the ProSPA instrument and adaptations to the experiment will be required.

The water release phase showed the pressure peaks are limited to ~16 mbar which is well within the linear pressure range (~80 mbar) as identified in the water calibration tests. When the calibration factor, *F*, was applied there was ≤0.3 mbar increase in the pressure value. This suggests that almost all the water released from the cold finger is being detected by the pressure sensor, and not condensing elsewhere in the system.

The series of experiments showed that the water yield to ilmenite mass ratio is not 1:1. The smaller samples produce more water per unit mass of ilmenite compared to the

larger samples. For example, a sample of 11.2 mg (25% of 44.7 mg) produced 55% of the amount of water produced by the 44.7 mg sample. It is possible that the smaller samples are not as compacted at the bottom of the ceramic tube as the larger samples, enabling greater movement of gases to and from the reaction sites. Both the reaction phase and water release phase data sets show that at > ~30 mg of sample the reaction does not appear to produce significantly more water. This suggests that within a static system hydrogen cannot penetrate below a certain depth. In this case, a 30 mg sample equates to a depth of ilmenite sample of ~2.3 mm with a defined grain size of ~ 170 μm. It is assumed that produced water cannot diffuse away quickly enough from below this depth and the reaction is suppressed. A delayed pressure rise in the system (Fig. 7a) during the water release phase suggests that water is initially released and re-condensed at a cold spot higher in the cold finger, which is as a result of thermal lag. Once the cold finger is uniformly heated, a significant release of volatiles is measured.

As seen in Fig. 8, a constant decrease in oxygen yield (as a wt. % of the original sample) with ilmenite mass shows that the smaller samples are closer to reaction completion than the larger samples. As no sample produced the maximum possible of 10.5 wt.% oxygen, it supports the idea that the reaction does not complete in 1 hour with the defined system characteristics. A higher reaction temperature and potentially longer reaction times should lead to higher yields when operating at these low pressures as more ilmenite is reduced.

The yield calculated from the drop in hydrogen pressure during the reaction is greater than the yield calculated from the vapor release from the cold finger. This suggests that not all the water produced during the reaction is condensed at the cold finger. One

major difference in the operational volume between the reaction phase and the water release phase, is that the furnace is only included in the reaction phase. Therefore, if water is trapping on cooler pipework between the hot furnace and the valve connecting it to the rest of the system, then this water would not be included in the yields measured in the water release phase. The trapping and releasing of water is on average ~68 % efficient when comparing the difference in pressure changes recorded in each phase. It is suggested that a future version of the BDM be built with increased thermal control to minimize such condensation of water in undesirable locations.

BSE images were used to identify metallic iron formation as an indicator of where the reaction has occurred. As the reacted grains do not show the presence of metallic iron in all areas, the reaction is likely incomplete, which was suggested from the pressure readings and yield calculations. The grains do not appear to have reacted uniformly in each ilmenite sample. Looking at a random selection of grains from each experiment shows that smaller samples reacted more completely than larger samples. Some grains appeared mostly unreacted, while others were extensively reacted, supporting the suggestion that reactants and products cannot move easily below a certain depth of ilmenite grains. It is not practical to select grains from the top or bottom of the sample holder specifically for this to be confirmed, as a result of the narrow dimensions of the sample holder. If the average ilmenite grain size were smaller, which could be the case on the lunar surface (McKay et al., 1991), the reaction rate would likely increase as the surface area increases, and the distance of gas diffusion required through the interior of the grains is reduced, although smaller grain sizes would also result in a longer diffusion pathway between grains. A wider sample holder, and/or smaller grain size could

potentially enable greater penetration of hydrogen gas into the sample, and quicker removal of water from the reaction site, potentially increasing the sample size limit of the reaction and increasing the reaction rate.

The reaction efficiency of the BDM is relatively low, producing up to 1.4 wt. % oxygen from relatively pure ilmenite. Meanwhile, other ISRU technologies such as PILOT and ROxygen could produce similar yields from regolith (Sanders and Larson, 2012). However, the reaction procedure used in this work was not optimized for greatest yields. The system successfully reduced iron bearing minerals to produce and collect water. The next steps will require optimization of the system and procedure so it is capable of reducing samples with lunar-like composition.

A lunar surface sample will likely contain ≤20 % by volume ilmenite, where a highland sample would likely have ≤1 % by volume ilmenite. Assuming a 45 mg lunar sample is collected into a ProSPA sized oven and contains 1 % ilmenite (~0.45 mg), a first order estimate can be made for the amount of water produced. First, based on the data in table 1, assume that the relationship between the amount of water produced and condensed at the cold finger n_w, and the mass of ilmenite, m_{ilm}, is a second order polynomial where $n_w=-1x10^{-5}m_{ilm}^2+9x10^{-4}m_{ilm}+0.0013$. Assuming that the presence and composition of other lunar minerals in the sample has no impact on the production of water from the ilmenite present, then ~1.7 µmol of water (0.06 wt. % oxygen yield) would be produced and condensed in 1 hour in the BDM system. A yield of this size equates to a pressure in the BDM system of ~ 1.7 mbar which is likely too small to be identifiable above a blank reading. The presence of lunar minerals will also likely slow down the movement of gases between grains, particularly if the ilmenite grains present

happen to be at the bottom of the sample or integrated into the matrix of other minerals in agglomerates. To improve these yields higher temperatures and longer reaction times would likely result in measurable yields. Also, other iron bearing lunar minerals can reduce including plagioclase and pyroxene, albeit at much lower efficiencies (Allen et al., 1994). As a result, low ilmenite concentrations may not be a barrier to the production and measurement of water from a lunar sample using a ProSPA-like system.

6 Conclusions

We have demonstrated that ilmenite can be reduced by hydrogen in a ProSPA-like static system operated at 900 °C for 1 hour, producing yields of up to 1.4±0.1 wt.% oxygen. Smaller samples react more fully, up to 12.9±1.5 % complete, as a result of the sample holder dimensions and reaction kinetics, as the reactants and products cannot easily move around the ilmenite grains. One of the implications of this work for ProSPA ISRU studies is the need for temperature control of the entire system if the extracted water is to be measured by its pressure in a closed system. This work has also highlighted the limitations of the current narrow/deep oven in a static (non-fluidized bed) configuration, currently estimating that there is a mass limit of ~30 mg (corresponding to a depth of ~2.3 mm) above which an increase in ilmenite mass does not result in an increase in water produced in the given time and at the given conditions. Although the system is not optimized for an ISRU reaction, it is a simple technique that can be used to perform a proof-of-principle reduction reaction of lunar ilmenite *in situ*.

Acknowledgements

The authors would like to acknowledge the support of Dr Giulia Degli-Alessandrini for assistance with operating the SEM, Dr Pallavi Anand for assistance with the Nikon SMZ1500 microscope and infinity capture software, and Dr Aiden Cowley for supplying the ilmenite used in the experiments. This work was supported by a Science and Technology Facilities Council (STFC) studentship grant [grant number ST/N50421X/1] to HS and by The Open University. ProSPA is being developed by a consortium led by The Open University, UK, under contract to the PROSPECT prime contractor Leonardo S.p.A., Italy, within a programme of and funded by the European Space Agency.

References

Allen, C. C., Morris, R. V., & McKay, D. S. (1994). Experimental reduction of lunar mare soil and volcanic glass. *Journal of Geophysical Research: Planets*, 99(E11), 23173-23185.

Altenberg, B., Franklin, H., & Jones, C. (1993). *Thermodynamics of lunar ilmenite reduction*. Paper presented at the Lunar and Planetary Science Conference XXIV, Houston, Texas.

Anand, M., Asher, Y., Buchwald, R., Carnelli, I., Carpenter, J., Conti, M., . . . Urbina, D. (2018). *Towards the use of lunar resources.* European Space Agency.

Barber, S., Smith, P., Wright, I., Abernethy, F., Anand, M., Dewar, K., . . . Morgan, G. (2017). *ProSPA: the Science Laboratory for the Processing and Analysis of Lunar Polar Volatiles within PROSPECT*. Paper presented at the 48th Lunar and Planetary Science, Houston, Texas.

Barber, S. J., Wright, I. P., Abernethy, F., Anand, M., Dewar, K. R., Hodges, M., . . . Trautner, R. (2018). *ProSPA: Analysis of Lunar Polar Volatiles and ISRU Demonstration on the Moon.* Paper presented at the 49th Lunar and Planetary Science Conference, Houston, Texas.

Buck, A. (1996). Buck Research CR-1A User's Manual. Buck Research Instruments: Boulder, CO, USA.

Chambers J. G., Taylor L. A., Patchen A., McKay D. S. (1995) Quantitative mineralogical characterization of lunar high-Ti mare basalts and soils for oxygen production. *Journal of Geophysical Research*, 100, 14391-14401. https://doi.org/10.1029/95JE00503

Christiansen, E., Simonds, C. H., & Fairchild, K. (1988). *Conceptual design of a lunar oxygen pilot plant*. LPI Contributions, 652, 52.

Dang, J., Zhang, G.-h., & Chou, K.-c. (2015). Kinetics and mechanism of hydrogen reduction of ilmenite powders. *Journal of Alloys and Compounds*, 619, 443-451. https://doi.org/10.1016/j.jallcom.2014.09.057

Delchar, T. A. (1993). *Vacuum physics and techniques*: Chapman and Hall.

Denk, T. (2018). *Full-Scale Terrestrial Demonstrator for ilmenite Reduction with Concentrated Solar Power*. Paper presented at the European Lunar Symposium, Toulouse, France.

ESA. (2018). *In-Situ Resource Utilisation (ISRU) demonstration mission*. Retrieved from http://exploration.esa.int/moon/60127-in-situ-resource-utilisation-demonstration-mission/. Accessed 19/08/2019.

ESA. (2015). *Exploring Together: ESA Space Exploration Strategy*. Retrieved from Strategic Planning and Outreach Office of the ESA Directorate of Human Spaceflight and Operations, ESTEC, PO Box 299 2200 AG Noordwijk The Netherlands.

Geankoplis, C. J. (1993). *Transport Processes and Unit Operations*. (3 ed.). Engelwood Cliffs, NJ: PTR Prentice-Hall.

Gibson, M. A., & Knudsen, C. W. (1985). *Lunar oxygen production from ilmenite.* Paper presented at the Lunar bases and space activities of the 21st century, Houston, TX.

Goldstein, J. I., Newbury, D. E., Michael, J. R., Ritchie, N. W., Scott, J. H. J., & Joy, D. C. (2017). *Scanning electron microscopy and X-ray microanalysis*: Springer.

Hallis L. J., Anand M., Strekopytov S. (2014) Trace-element modelling of mare basalt parental melts: Implications for a heterogeneous lunar mantle. *Geochimica et Cosmochimica Acta,* (134) 289-316. https://doi.org/10.1016/j.gca.2014.01.012

ISECG, I. S. E. C. G. (Producer). (2018). *The Global Exploration Roadmap*. Retrieved from https://www.nasa.gov/sites/default/files/atoms/files/ger_2018_small_mobile.pdf

Linne, D., Kleinhenz, J., & Hegde, U. (2012). *Evaluation of Heat Recuperation in a Concentric Hydrogen Reduction Reactor*. Paper presented at the 50th AIAA Aerospace Sciences Meeting including the New Horizons Forum and Aerospace Exposition, Nashville, TN.

Linne, D. L., Gokoglu, S., Hegde, U. G., Balasubramaniam, R., & Santiago-Maldonado, E. (2009*). Component and System Sensitivity Considerations for Design of a Lunar ISRU Oxygen Production Plant*. Paper presented at the 47th AIAA Aerospace Sciences Meeting including The NewHorizons Forum and Aerospace Exposition, Orlando, Fl.

Lomax, B., Conti, M., Khan, N., Ganin, A., & Symes, M. (2019). *The Metalysis-FCC-Cambridge process for efficient production of oxygen and metals on the lunar surface.* Paper presented at the European Lunar Symposium, Manchester, UK.

McKay, D. S., Heiken, G., Basu, A., Blanford, G., Simon, S., Reedy, R., . . . Papike, J. (1991). *The lunar regolith*. Lunar sourcebook, 285-356 (pg. 289)

Meyen, F. E., Hecht, M. H., & Hoffman, J. A. (2016). Thermodynamic model of Mars Oxygen ISRU Experiment (MOXIE). *Acta Astronautica,* 129, 82-87. doi:10.1016/j.actaastro.2016.06.005

Papike, Taylor, L., & S, S. (1991). *Lunar Minerals*. In G. Heiken, D. Vaniman, & B. M. French (Eds.), Lunar sourcebook (pp. 121-181).

Pfeiffer Vacuum, G. (2013). *Vacuum technology book* (Vol. II). Asslar, Germany: Pfeiffer Vacuum GmbH.

Rao, D. B., Choudary, U., Erstfeld, T., Williams, R. J., & Chang, Y. (1979). Extraction processes for the production of aluminum, titanium, iron, magnesium, and oxygen and nonterrestrial sources. In J. Billingham, W. Gilbreth, and B. O'Leary (Eds.) *Space Resources and Space Settlements* NASA SP-428, pp. 257-274.

Sanders G. B. & Larson, W. E. (2011). Integration of in-situ resource utilization into lunar/Mars exploration through field analogs. *Advances in Space Research*, 47(1), (20-29).

Sanders, G. B., & Larson, W. E. (2012). Progress made in lunar in situ resource utilization under NASA's exploration technology and development program. *Journal of Aerospace Engineering*, 26(1), 5-17.

779 Talboys, D., Barber, S., Bridges, J., Kelley, S., Pullan, D., Verchovsky, A., . . . Pillinger,
780 C. (2009). In situ radiometric dating on Mars: Investigation of the feasibility of K-Ar
781 dating using flight-type mass and X-ray spectrometers. *Planetary and Space Science*,
782 57(11), 1237-1245.
783 Taylor, L., & Carrier, W. (1993). Oxygen Production on the Moon: An Overview and
784 Evaluation. In J. S. Lewis, M. S. Matthews, & M. L. Guerrieri (Eds.), *Resources of Near-*
785 *Earth Space* : University of Arizona Press pp. 69-108.
786 Taylor, L. A., Jerde, E. A., McKay, D. S., Gibson, M. A., Knudsen, C. W., & Kanamori,
787 H. (1993). *Production of O_2 on the Moon: A lab-top demonstration of ilmenite reduction*
788 *with hydrogen*. Paper presented at the Lunar and Planetary Science Conference XXIV,
789 Houston, Texas.
790 Taylor, L. A., Pieters, C., Patchen, A., Taylor, D. H. S., Morris, R. V., Keller, L. P., &
791 McKay, D. S. (2010). Mineralogical and chemical characterization of lunar highland
792 soils: Insights into the space weathering of soils on airless bodies. *Journal of*
793 *Geophysical Research: Planets*, 115(E2). https://doi.org/10.1029/2009JE003427
794 Trimble, J., & Carvalho, R. (2016). *Lunar prospecting: searching for volatiles at the*
795 *south pole*. Paper presented at the 14th International Conference on Space Operations,
796 Daejeon, Korea. https://doi.org/10.2514/6.2016-2482
797 Tuzi, Y., Tanaka, T., Takeuchi, K., & Saito, Y. (1996). Effect of surface treatment on the
798 adsorption kinetics of water vapor in a vacuum chamber. *Vacuum*, 47(6-8), 705-708.
799 Warner R. D., Nehru C. E., Keil K. (1978) Opaque oxide mineral crystallization in lunar
800 high-titanium mare basalts. *American Mineralogist* 63, 1209-1224.

Williams, R. J., McKay, D. S., Giles, D., & Bunch, T. E. (1979). Mining and beneficiation of lunar ores. In J. Billingham, W. Gilbreth, and B. O'Leary (Eds.) *Space Resources and Space Settlements* NASA SP-428, pp. 275-188.

Williams, R. J., & Mullins, O. (1983). *Enhanced production of water from ilmenite: An experimental test of a concept for producing lunar hydrogen*. Paper presented at the Lunar and Planetary Science XIV, Special Session Abstracts, Lunar and Planetary Institute, Houston.

Wright, I., Barber, S., Morgan, G., Morse, A., Sheridan, S., Andrews, D., . . . Leese, M. (2007). Ptolemy–an instrument to measure stable isotopic ratios of key volatiles on a cometary nucleus. *Space Science Reviews*, 128(1-4), 363-381.

Zhao, Y., & Shadman, F. (1993). Production of Oxygen from Lunar Ilmenite. In J. S. Lewis, M. S. Matthews, & M. L. Guerrieri (Eds.), *Resources of Near-Earth Space* (pp. 149-178): University of Arizona Press.

Conflict of Interest statement

This work was supported by a Science and Technology Facilities Council (STFC) studentship grant [grant number ST/N50421X/1] to HS and by The Open University. ProSPA is being developed by a consortium led by The Open University, UK, under contract to the PROSPECT prime contractor Leonardo S.p.A., Italy, within a programme of and funded by the European Space Agency.